Independent and interactive roles of hirudin and HMGB1 interference in protecting renal function by regulating autophagy, apoptosis, and kidney injury in chronic kidney disease

Ying Li,[1,2]* Xuan Gao,[3]* Yao Chen,[4] Huihui Li,[3] Jing Tang,[3] Wei Sun[1,2]

[1]Nanjing University of Chinese Medicine, Nanjing, Jiangsu
[2]Department of Nephrology, Jiangsu Province Hospital of Chinese Medicine (Affiliated Hospital of Nanjing University of Chinese Medicine), Nanjing, Jiangsu
[3]Department of Nephrology, Chongqing Traditional Chinese Medicine Hospital, Chongqing
[4]Department of Pediatrics, the First Affiliated Hospital of the Army Military Medical University (Southwest Hospital), Chongqing, China

*These authors contributed equally to this work.

ABSTRACT

Chronic kidney disease (CKD) is a progressive disorder characterized by renal fibrosis, inflammation, and dysregulated autophagy and apoptosis. High-mobility group box 1 (HMGB1) plays a crucial role in regulating autophagy in CKD. Hirudin, a potent thrombin inhibitor, has demonstrated antifibrotic and anti-inflammatory properties, but its effects on autophagy and apoptosis in CKD remain unclear. In this study, a rat model of renal interstitial fibrosis (RIF) and an HK-2 cell culture model were established to assess the effects of varying doses of hirudin and HMGB1 interference. Molecular and histological analyses, including RTqPCR, Western blot, TUNEL staining, hematoxylin-eosin (H&E) staining, immunofluorescence, and immunohistochemistry (IHC), were performed to assess renal injury, fibrosis, apoptosis, and autophagy-related markers. Hirudin treatment significantly reduced the expression of LC3, ATG12, ATG5, α-SMA, COL1A1, caspase-3, and caspase-9 while increasing P62 levels ($p<0.05$). It also lowered the renal coefficient ($p<0.001$) and apoptosis levels. The optimal effective concentration of hirudin *in vitro* was determined to be 4.8 ATU/mL ($p<0.001$). HMGB1 interference suppressed autophagy and apoptosis, as indicated by decreased LC3-II/LC3-I, ATG12, ATG5, caspase-3, and caspase-9 levels, increased P62 expression ($p<0.001$), and reduced apoptosis. However, simultaneous HMGB1 interference in hirudin-treated cells weakened the therapeutic effects of hirudin, leading to increased autophagy and apoptosis markers, decreased P62 levels, and a higher renal coefficient. These findings indicate that hirudin exerts protective effects in CKD by modulating autophagy and apoptosis, potentially through HMGB1 regulation. These findings highlight the therapeutic potential of targeting these mechanisms in renal dysfunction and underscore the necessity for further research to support clinical applications.

Key words: hirudin; chronic kidney disease; autophagy; apoptosis, HMGB1.

Correspondence: Wei Sun, Department of Nephrology, Jiangsu Province Hospital of Chinese Medicine (Affiliated Hospital of Nanjing University of Chinese Medicine), Nanjing, Jiangsu Province, China.
E-mail: jssunwei@163.com

Contributions: YL, conceptualization, data curation, funding acquisition, manuscript original draft; YC, conceptualization, data curation, manuscript original draft; HL, JT, investigation, resources, supervision; WS, formal analysis, project administration, manuscript review and editing; XG, methodology, validation, visualization, manuscript review and editing. All authors read and approved the final version of the manuscript and agreed to be accountable for all aspects of the work.

Conflict of interest: the authors declare no conflict of interest regarding the present study.

Ethical approval: all experimental protocols were approved by the Animal Ethics Committee of the Chongqing Traditional Chinese Medicine Hospital (2023-ky-10). All methods were carried out in accordance with relevant guidelines and regulations. All methods are reported in accordance with the ARRIVE guidelines.

Availability of data and materials: the data used to support the findings of this study are available from the corresponding author upon reasonable request.

Funding: this research was supported by Chongqing Natural Science Foundation (CSTB2022NSCQ-MSX0413 and cstc2021jcyj-msxmX0759), Joint Project of Chongqing Health Commission and Science and Technology Bureau (2023ZDXM002).

Introduction

Chronic kidney disease (CKD) refers to kidney damage or decline in renal function caused by various causes that last for 3 months or more, and can develop into end-stage kidney disease.[1] CKD, is a global health problem, with a prevalence of 10% to 14% in many countries worldwide, and it is on the rise,[2] posing a serious threat to the quality of life and survival of patients. The development mechanism of CKD encompasses intricate biological processes, including glomerular hypertension, renin-angiotensin-aldosterone system signaling, podocyte equilibrium, dyslipidemia, renal tubulointerstitial fibrosis, as well as inflammatory response,[3] which may be influenced by genetic, environmental, and lifestyle factors, resulting in a gradual deterioration of renal function.[4] Present data indicates that autophagy plays a role in CKD progression, and autophagy loss causes immune inflammation, resulting in further impaired renal function.[5] Autophagy is a cyclic process in which cells degrade and reconstruct impaired organelles and proteins, a crucial function in preserving cellular equilibrium and organ operation.[6] Nonetheless, the precise mechanism of autophagy malfunctions in CKD remains uncertain, necessitating further investigation to uncover novel potential treatment objectives. The degree of renal tubulointerstitial disease is the primary indicator for assessing the deterioration of kidney function and predicting the prognosis.[7] As the extent of renal interstitial fibrosis (RIF) is closely linked to the level of kidney injury, and initial RIF can be wholly reversed, researching potent anti-fibrotic medications to revert early lesions holds significant importance for the prediction of kidney disease.[8] Lately, Chinese medicine researchers have conducted a lot of exploratory studies on the prevention and treatment of renal tubulointerstitial fibrosis, and have shown good clinical efficacy, but there are some problems. Traditional Chinese medicine, especially the drugs for enhancing blood flow and eliminating blood stagnation, has been extensively utilized in medical studies on the on preventing and treating renal tubulointerstitial fibrosis.[9-12] However, the efficacy and mechanism of different types and dosages of medications for enhancing blood flow and eliminating blood stagnation remain unclear. Hirudin, the primary active ingredient of Chinese medicine *Hirudo nipponica* Whitman, has been proved to be an effective thrombin specific inhibitor in clinical and experimental studies,[13] and has anti-coagulation, anti-thrombosis, anti-inflammation, anti-fibrosis and other effects.[14] Research indicates that hirudin can notably downregulate the level of fibrin gene, inhibit the number of cytokines secreted by mesangial cells, and delay RIF progression.[15] Lately, hirudin has been employed to treat glomerulosclerosis, diabetic nephropathy, hypertensive nephropathy, and additional CKDs.[15-17] This provides a preliminary experimental foundation for using hirudin in CKD treatment. However, the exact mechanism of hirudin's role in treating CKD and its interaction with other signaling pathways still need to be further explored. High mobility group protein 1 (HMGB1) is a nuclear protein that performs a crucial function in cell injury and inflammatory responses.[18] Research has demonstrated that HMGB1 is implicated in the onset and progression of various kidney conditions, such as ischemia-reperfusion injury, CKD and renal fibrosis, diabetic nephropathy, and granulomatous nephritis.[19] Studies have shown that there is a complex interaction between HMGB1 and autophagy and inflammatory response.[20] Tang *et al*.[21] discovered that HMGB1 in a reducible state induces autophagy, whereas HMGB1 in an oxidized state stimulates cancer cell apoptosis. Therefore, this study aimed to examine the effects of the hirudin and HMGB1 on autophagy and CKD, as well as to identify new treatment objectives and strategies for the treatment of CKD, which is expected to bring innovative breakthroughs for the treatment and management of CKD.

Materials and Methods

Animal model construction and grouping

Specific pathogen free (SPF)-grade male SD rats were obtained from Ensiweier company (Chongqing, China). The rats were randomly assigned into the following groups: sham group, model group (unilateral ureteral obstruction, UUO), low-dosage hirudin group (UUO+hirudin-L), medium-dosage hirudin group (UUO+hirudin-M), high-dosage hirudin group (UUO+hirudin-H), Negative Control (NC) group, sh NC group, sh HMGB1 group, Hirudin+sh NC group, and Hirudin+sh HMGB1 group, with 9 rats in each group. The UUO model was used to induce RIF. All rats received anesthesia with 2% pentobarbital sodium (P3761, BSZH Scientific, Beijing, China) after modeling. A longitudinal cut was performed expose the left kidney and locate the left ureter. The upper and lower segments of the ureter were tied near the renal pelvis and about a third from the top, individually. Rats in the low, medium, and high dose groups were treated with 0.7 g/kg.d, 1.4 g/kg.d, 2.8 g/kg.d hirudin by gavage. Rats in the sham and model groups were given normal saline by gavage. The AAV-shRNA-HMGB1 plasmids were constructed by Biomedicine Company (Chongqing, China). The NC group, sh NC group, sh HMGB1 group, Hirudin+sh NC group, and Hirudin+sh HMGB1 group were established. The plasmid was administered into the renal artery three weeks in advance. The body weight of the rats was recorded weekly. At 21 days post-modeling, the animals in each group were euthanized under anesthesia with pentobarbital sodium. The kidneys were dissected, weighed after cleaning, and some parts were processed for paraffin sections and treated with 4% paraformaldehyde at room temperature for 6 h, while the remaining samples were stored at -80°C.

Cell culture and grouping

HK-2 cells were obtained from the American Type Culture Collection (ATCC) and subsequently passaged and maintained in Dulbecco's modified eagle medium/nutrient mixture F-12 (DMEM/F12) medium (L310KJ, Basalmedia Biotechnology, Shanghai, China) containing 10% fetal bovine serum (FBS) (AC03L055, Li Ji Biological, Shanghai, China) and 1% penicillin-streptomycin (C0009, Beyotime, Shanghai, China) at cell culture incubator. After resuscitation, the cells were expanded and cultured in serum-free DMEM/F12 medium under a tri-gas condition (5% CO_2, 1% O_2, 94% N_2) at 37°C for 24 h, followed by a switch to complete culture medium for 12 h to establish a hypoxia-reoxygenation model in an incubator with 5% CO_2, 21% O_2, and 74% N_2. The cells were then divided into groups according to different concentrations of hirudin: 0.3 ATU/mL, 0.6 ATU/mL, 1.2 ATU/mL, 2.4 ATU/mL, 4.8 ATU/mL, and 9.6 ATU/mL.[22] After 72 h of reoxygenation, hirudin at different concentrations was introduced to respective group, and the cells were further incubated for 48 h for subsequent sample collection and testing.

The cells were randomly assigned to the following groups: control (CTL) group (as a negative control), Hirudin group, sh NC group, sh HMGB1 group, Hirudin+sh NC group, and Hirudin+sh HMGB1 group. The shRNA plasmids were constructed by Biomedicine Company (Chongqing, China). For the sh NC and sh HMGB1 groups, after expansion and passage, HK-2 cells were transfected with empty shRNA plasmids and shRNA plasmids containing HMGB1 using transfection reagent MAX (10668-012, Biomedicine, Chongqing, China) to construct the model. The CTL group cells were incubated normally in medium without hirudin. Within the Hirudin group, the cells were exposed to 4.8 ATU/mL hirudin following 72 h of reoxygenation. In the Hirudin+sh NC

and Hirudin+sh HMGB1 groups, following 72 h of reoxygenation, the cultured cells were exposed to 4.8 ATU/mL hirudin for 48 h before transfection with plasmids. Following another 24 h of culture, samples were gathered for testing.

Cell counting kit-8

Cells from each group were placed into a 96-well plate and incubated for 12 h, after which 10 µL of CCK-8 solution (C0038, Beyotime, Shanghai, China) was added to each well. The plate was then placed in incubator for 4 h. Subsequently, the optical density (OD) at 450 nm was measured using a microplate spectrophotometer (CMax Plus, Molecular Devices, San Jose, CA, USA). Cell viability (100%) = (OD experimental group - OD blank group) / (OD control group - OD blank group) × 100%.

Experimental group: OD of cells with overexpressed or interfered plasmids and CCK-8 solution. Blank group: OD of wells containing culture medium and CCK-8 solution sans cells. Control group: OD of wells containing empty-loaded cells and CCK-8 solution.

RNA extraction and RTqPCR

Total RNA extraction was performed using TRIzol reagent (Thermo Fisher Scientific, Inc., Waltham, MA, USA).[23] Subsequently, reverse transcription was performed utilizing the Goldenstar™ RT6 cDNA Synthesis Kit Ver.2 (TSK302M, Tsingke Biotechnology Co., Ltd., Beijing, China) with the conditions: 25°C for 10 min, 55°C for 30 min, and 85°C for 5 min. The relative level of mRNA was detected utilizing the 2×T5 Fast qPCR Mix (SYBR Green I) assay kit (TSE002, Tsingke Biotechnology Co., Ltd., China) under the following reaction conditions: 95°C for 30 s, 95°C for 5 s, 60°C for 30 s, for 40 cycles. Human glyceraldehyde-3-phosphate dehydrogenase (GAPDH) served as the internal control, and the relative level was determined employing the $2^{-\Delta\Delta Ct}$ method. The sequences of the primers used are reported in Table 1.

Western blot analysis

Radioimmunoprecipitation assay (RIPA) lysis buffer comprising phenylmethylsulfonyl fluoride (PMSF) and protease inhibitor cocktail (P0013B, Beyotime) was added to the cells or ground kidney tissue to extract total protein. Five-hundred µg of total protein from each specimen was blended with 5× SDS loading buffer at a proportion of 4:1, resulting in a final concentration of 3.3 µg/µL, and subsequently warmed at 100°C for 6 min to denature the proteins. The proteins were separated *via* 10% sodium dodecyl sulfate-polyacrylamide gel flectrophoresis (SDS-PAGE) for 90 min and then shifted to a Polyvinylidene Fluoride (PVDF) membrane. These membranes were then blocked with 5% skim milk at 25°C for 1 h and then soaked with primary antibodies at 4°C overnight. The following day, after incubating with HRP goat anti-rabbit IgG (H+L) (AS014, ABclonal Technology, Wuhan, China) for 1 h at room temperature, the ECL exposure mixture (34580, Thermo Fisher Scientific, Inc.) was uniformly applied to the PDVF. Finally, the bands were detected by a nucleic acid and protein gel imaging system (Bio-Rad Laboratories, Hercules, CA, USA). The band strength was determined using ImageJ program (version 1.48b, National Institutes of Health, Bethesda, MD, USA). Primary antibodies against LC3 (A12319, 1:1000), ATG12 (A15609, 1:1000), ATG5 (A0203, 1:1000), P62 (A19700, 1:20000), and GAPDH (A19056, 1:50000) were purchased from ABclonal.

TUNEL assay for apoptosis detection

After dewaxing and rehydrating paraffin-embedded sections of mouse kidney, the sections were rinsed with PBS and incubated with a proper quantity of Proteinase K working mix. Then, 3% H_2O_2 (prepared in PBS) was added to the tissue, followed by Tunel staining according to the instructions of as per the guidelines of the 3,3'-diaminobenzidine (DAB) (SA-HRP) Tunel Cell Apoptosis Detection Kit (G1507, Servicebio, Wuhan, China). The cell nuclei were dyed with hematoxylin (G1004, Servicebio), dehydrated, and mounted with neutral resin (10004160, Sinopharm, Beijing, China). For fixed HK-2 cell slides, an appropriate amount of 0.3% Triton X-100 permeabilization solution was applied to the slides and incubated at ambient conditions for 5 min. Tunel staining was carried out using a one-step TUNEL assay kit (CY3 red fluorescence) following the manufacturer's directions, followed by nuclear dyeing with DAPI (C1005, Beyotime) and mounting with anti-fluorescence quenching reagent (P0126, Beyotime). Photographs of the segments were taken utilizing an Mshot inverted microscope (MF53, Mingtai Optical Technology Co., Ltd., Guangzhou, China).

Hematoxylin and eosin (H&E) staining

The kidney tissue was rinsed with PBS, fixed in 4% paraformaldehyde, then immersed in 75%, 85%, 95%, and 100% ethanol for 2 h each, cleared with xylene for 20 min, and embedded in paraffin. 2.5 µm thick sections were heated in an oven at 55°C then deparaffinized, rehydrated in graded ethanol, rinsed three times with double distilled water, and stained with hematoxylin (G1004, Servicebio) for 3 min; the excess staining was rinsed with tap water and the sections were then stained with eosin (G1002, Servicebio). The tissues were subsequently dehydrated with 95% ethanol for 2 min and finally dehydrated with absolute ethanol for 2 min. Following xylene transparency for 5 min, the slides were sealed with neutral resin (10004160, Sinopharm, China), and photographed using Mshot MF53 microscope from Micro-shot Technology Co., Ltd. (Guangzhou, China).

Table 1. Primer sequence.

Primer	Sequence (5' to 3')
r-LC3-F	CCAGGATTCAGCACCAGATGT
r-LC3-R	CCTTGGCTACCTGGACTGTT
r-ATG12-F	AAGCAAGATGGCAGAAGACC
r-ATG12-R	TCGATGAGTGCTTGGACAGT
r-ATG5-F	GTGATCCCGGTAGACCCAAC
r-ATG5-R	GCCAAACTTCTTGCTCCCGA
r-P62-F	GAGGCACCCCGTAAAGTCAT
r-P62-R	GATTCAACCGCCATGTGCTT
r-GAPDH-F	TGGTGCTGAGTATGTCGTGG
r-GAPDH-R	GGCGGAGATGATGACCCTTT
h-LC3-F	TTGGTCAAGATCATCCGGCG
h-LC3-R	CCTCGTCTTTCTCCTGCTCG
h-ATG12-F	AGCGAACACGAACCATCCAA
h-ATG12-R	GGTCTGGGGAAGGAGCAAAG
h-ATG5-F	TGCAGTGGCTGAGTGAACAT
h-ATG5-R	TCTGTTGGCTGTGGGATGAT
h-P62-F	AGATTCGCCGCTTCAGCTT
h-P62-R	AACCAAGTCCCCGTCCTCAT
h-GAPDH-F	TCAAGGCTGAGAACGGGAAG
h-GAPDH-R	TCGCCCCACTTGATTTTGGA

LC3, microtubule-associated protein 1A/1Bight chain 3; ATG12, autophagy-related protein 12; ATG5, autophagy-related protein 5; p62, sequestosome-1.

Immunofluorescence analysis

Paraffin sections of renal tissues were dewaxed and rehydrated, and then rinsed 3 times with double-distilled water. Subsequently, the sections were immersed in citrate buffer (pH 6.0) or Tris-EDTA buffer (pH 9.0) for antigen retrieval. Microwave or pressure cooker heating was used for treatment (for citrate buffer: microwave heating at high power for 3 min, followed by standing for 5 min, and repeating once; pressure cooker heating for 3.5 min). After the retrieval, the sections were rinsed 3 times with PBS buffer for 1 min each time. Meanwhile, the fixed cell slides were taken out and rinsed 3 times with PBS. Both the sections and cell slides were added with 5% goat serum (C0265, Beyotime) and incubated at room temperature for 30 min for blocking. Subsequently, antibodies against α-smooth muscle actin (α-SMA, A2235, ABclonal), caspase-3 (A11319, Aibote, China), or caspase-9 (A0281, ABclonal) (dilution ratio 1:200) were added respectively, and incubated overnight at 4°C. As a negative control, a group of sections or cell slides was set up without the primary antibody, and only non-immune IgG of the corresponding species (dilution ratio 1:200) was added to exclude background signals from non-specific binding. After that, Cy3-labeled goat anti-rabbit IgG (H+L) secondary antibody (AS007, ABclonal) (dilution ratio 1:200) was added and incubated in the dark at 25°C for 1.5 h. Then, DAPI (C1005, Beyotime) staining solution was added and incubated in the dark for 5 min. Subsequently, the sections were rinsed 3 times with PBS to remove the excess DAPI staining solution. Finally, the sections were mounted with an anti-fluorescence quenching agent (P0126, Beyotime), and observed and photographed using an inverted fluorescence microscope (ICX41; Sunny Optical Technology (Group) Co., Ltd., China).

Positive evaluation methods include: using ImageJ software to quantitatively analyze the fluorescence signals, measuring the mean fluorescence intensity or the integrated density of the region of interest; counting the number of DAPI-labeled cell nuclei and Cy3-labeled positive cells in each field of view, and calculating the proportion of positive cells (number of positive cells / total number of cells × 100); if applicable, performing co-localization analysis and calculating the co-localization coefficient (such as the Pearson correlation coefficient) of different fluorescence signals. The specificity of the experimental results was verified by comparing the fluorescence intensity or the proportion of positive cells between the experimental group and the negative-control group.

Immunohistochemistry (IHC)

Paraffin sections of renal tissues were dewaxed and rehydrated, rinsed 3 times with double-distilled water, and then immersed in citrate buffer (pH 6.0) or Tris-EDTA buffer (pH 9.0) for antigen retrieval. Microwave or pressure cooker heating was used for treatment, as reported above, then the sections were rinsed 3 times with PBS buffer for 1 min each time. The sections were treated with 3% hydrogen peroxide at room temperature for 15 min to block the activity of endogenous peroxidase, and then rinsed 3 times with PBS. Subsequently, 5% goat serum (C0265, Beyotime) was added and incubated at room temperature for 60 min to block non-specific binding sites. Then, antibodies against caspase-3 (A11319, ABclonal), caspase-9 (A0281, ABclonal), or type I collagen (collagen I, A1352, ABclonal) (dilution ratio 1:200) were added and incubated overnight at 4°C. As a negative control, a group of sections was set up without the primary antibody, and only non-immune IgG of the corresponding species (dilution ratio 1:200) was added to exclude background signals from non-specific binding. After that, HRP-labelled goat anti-rabbit IgG (H+L) secondary antibody (A0208, Beyotime) (dilution ratio 1:50) was added and incubated at room temperature for 1.5 h. DAB chromogen solution (ZLI - 9019, ZSGB - BIO, Beijing) was added and incubated in the dark for 1 min, and then rinsed with tap water for 5 min. The sections were stained with hematoxylin (G1004, Servicebio) for 1 min, differentiated in 1% hydrochloric acid-ethanol solution for 2 s, and then rinsed with tap water for 10 min. The sections were dehydrated twice in 95% ethanol for 2 min each time, then immersed twice in xylene for 5 min each time, and finally mounted with a mounting medium.

Positive evaluation methods include: scoring the staining intensity according to the depth of DAB staining (0, no staining; 1, weak positive; 2, moderate positive; 3, strong positive); randomly selecting 5-10 fields of view under the microscope, counting the number of positive cells and the total number of cells, and calculating the proportion of positive cells (number of positive cells / total number of cells × 100); performing a comprehensive score by combining the staining intensity and the proportion of positive cells (H-score = staining intensity × proportion of positive cells). The specificity of the experimental results was verified by comparing the staining intensity or the proportion of positive cells between the experimental group and the negative control group.

Statistical analysis

The statistical analysis in this study utilized a Student's *t* test. The results are presented the mean ±SD. A significance level of $p<0.05$ denoted significant difference, with * indicating $p<0.05$. GraphPad Prism 8.0 (GraphPad Company, San Diego, CA, USA) was utilized for conducting one-way analysis of variance and Tukey's multiple comparisons test, with a significance threshold of $p< 0.05$.

Results

Efficacy validation of hirudin

The efficacy of hirudin was verified through *in vivo* experiments. The levels of genes and proteins associated with autophagy in renal tissues were identified utilizing RTqPCR and WB experiments (Figure 1 A,B). Compared to the sham group, the UUO group exhibited a significant increase in the expression of LC3, ATG12, and ATG5, accompanied by a notable decrease in P62 expression ($p<0.001$). Furthermore, in comparison with the UUO group, the UUO+low, medium, and high-dose hirudin groups showed a decrease in the expression of LC3, ATG12, and ATG5 with increasing concentration of hirudin, with the highest reduction observed in the high-dosage hirudin group. Conversely, P62 expression demonstrated an opposite trend ($p<0.0001$). The renal coefficient significantly increased in the UUO group (0.96%) compared to the sham group (0.71%) ($p<0.0001$), whereas it notably decreased in the UUO+low, medium, and high dose hirudin groups (0.86%, 0.81%, 0.76%) compared to the UUO group ($p<0.0001$) (Figure 1C). TUNEL staining indicated a notable elevation in apoptotic cells in the UUO group in comparison with the sham group, while the quantity of apoptotic cells in the UUO+low, medium, and high dose hirudin groups was markedly diminished in contrast to the UUO group (Figure 1D). Additionally, immunofluorescence and IHC results revealed that the levels of α-SMA, COL1A1, caspase-3, and caspase-9 in the UUO group were significantly higher than those in the sham group. Compared to the UUO group, the levels of α-SMA, COL1A1, caspase-3, and caspase-9 in the UUO+low, medium, and high-dose hirudin groups decreased with increasing concentration, with the highest reduction observed in the high dose hirudin group (Figure 2A). The above findings imply that hirudin may exert certain efficacy in CKD by regulating the process of cellular autophagy and reducing cell apoptosis. The results of HE staining showed that the renal tubules in the NC

group were dilated, indicating significant kidney injury. In the Hirudin group, there was slight dilation of the renal tubules, reduced interstitial fibrosis, and decreased infiltration of inflammatory cells. Compared to the UUO group, the degree of renal tubule dilation in the UUO+ low, medium, and high-dose Hirudin groups decreased with increasing concentration, along with reduced interstitial fibrosis and infiltration of inflammatory cells (Figure 2B).

Cell hirudin concentration screening

HK-2 cells were exposed to diverse hirudin concentrations to identify the most effective concentration. Results from the CCK-8 assay revealed that compared to 0.3 ATU/mL of hirudin, the viability of HK-2 cells increased with rising hirudin concentration, peaking at 4.8 ATU/mL, and decreased when the concentration reached 9.6 ATU/mL ($p<0.001$) (Figure 3A). Therefore, 4.8 ATU/mL was determined to be the optimal effective concentration of hirudin.

In vitro study on the effect of hirudin and HMGB1 on CKD

The results from RTqPCR and WB experiments revealed that compared to the CTL group, hirudin significantly reduced the expression of LC3, LC3-II/LC3-I ratio, ATG12, and ATG5 in HK-2 cells, while increasing the expression of P62 ($p<0.0001$)

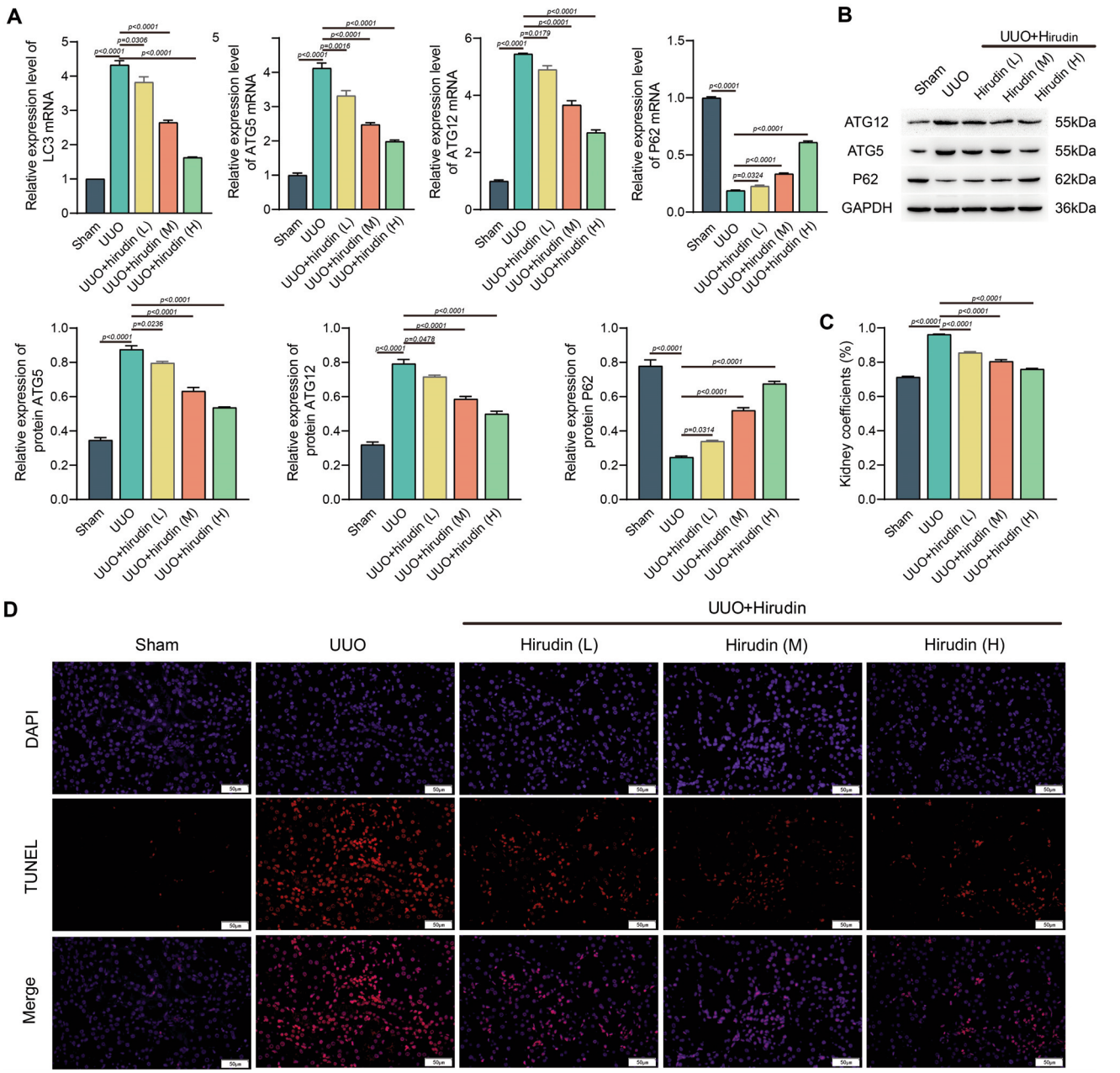

Figure 1. Effect of hirudin on autophagy and apoptosis in UUO rats. **A**) Expression of LC3, ATG12, ATG5 and P62 mRNA in UUO rat kidney tissue was observed by RTqPCR. **B**) Western blot analysis of ATG12, ATG5 and P62 protein expression in UUO rat kidney tissue. **C**) UUO rat renal co-efficiency. **D**) TUNEL detected apoptosis in renal tissues.

(Figure 3 B,C). In comparison to the sh NC group, HMGB1 interference notably decreased the levels of LC3, LC3-II/LC3-I, ATG12, and ATG5, while increasing P62 expression (p<0.0001). However, in CKD cells treated with both HMGB1 interference and hirudin togather, autophagy and apoptosis markers increased i.e LC3, ATG12, and ATG5, while P62 levels decreased, , compared to the Hirudin group (p<0.0001). TUNEL results indicated that the red fluorescence in the Hirudin group was significantly lower than that in the CTL group, and the red fluorescence in the sh HMGB1 group was notably lower than that in the sh NC group, suggesting that both hirudin and HMGB1 interference could inhibit cell apoptosis. Furthermore, compared to the Hirudin group, cell apoptosis was significantly increased in the Hirudin+sh HMGB1 group (Figure 3D). Immunofluorescence results (Figure 3E) demonstrated that compared to the CTL group, the protein levels of caspase-3 and caspase-9 were reduced in the Hirudin group. The levels of caspase-3 and caspase-9 in the sh HMGB1 group were notably lower than those in the sh NC group. In contrast, compared to the Hirudin group, the Hirudin+sh HMGB1 group exhibited a notable increase in the levels of caspase-3 and caspase-9. These findings suggest that hirudin and HMGB1 can regulate the process of cellular autophagy, reduce cell apoptosis, and that interference with HMGB1 diminishes the therapeutic efficacy of hirudin.

An *in vivo* study of hirudin and HMGB1 in CKD rats

The results from RTqPCR and WB experiments showed that compared to the NC group, hirudin significantly reduced the levels of LC3, LC3-II/LC3-I ratio, ATG12, and ATG5 in rats, while increasing the expression of P62 (p<0.0001). Compared to the sh NC group, interference with HMGB1 significantly reduced the levels of rat LC3, LC3-II/LC3-I, ATG12, and ATG5, while increasing P62 expression (p<0.0001). Moreover, compared to the Hirudin group, simultaneous interference with HMGB1 expression significantly increased the levels of LC3, LC3-II/LC3-I, ATG12, and ATG5, while decreasing P62 expression (p<0.0001) (Figure 4 A,B). Furthermore, we compared the renal coefficient and found that compared to the NC group, hirudin significantly reduced the renal coefficient in rats (p<0.0001), while the renal coefficient in the sh HMGB1 group was significantly lower than that in the sh NC group (p=0.0005). The renal coefficient in the Hirudin+sh HMGB1 group was significantly higher than that in the Hirudin group (p=0.0054) (Figure 4C) TUNEL results indicated that the red fluorescence in the Hirudin group was significantly lower than that in the NC group, and the red fluorescence in the sh HMGB1 group was significantly lower than that in the sh NC group, suggesting that hirudin and interference with HMGB1 can inhibit cell

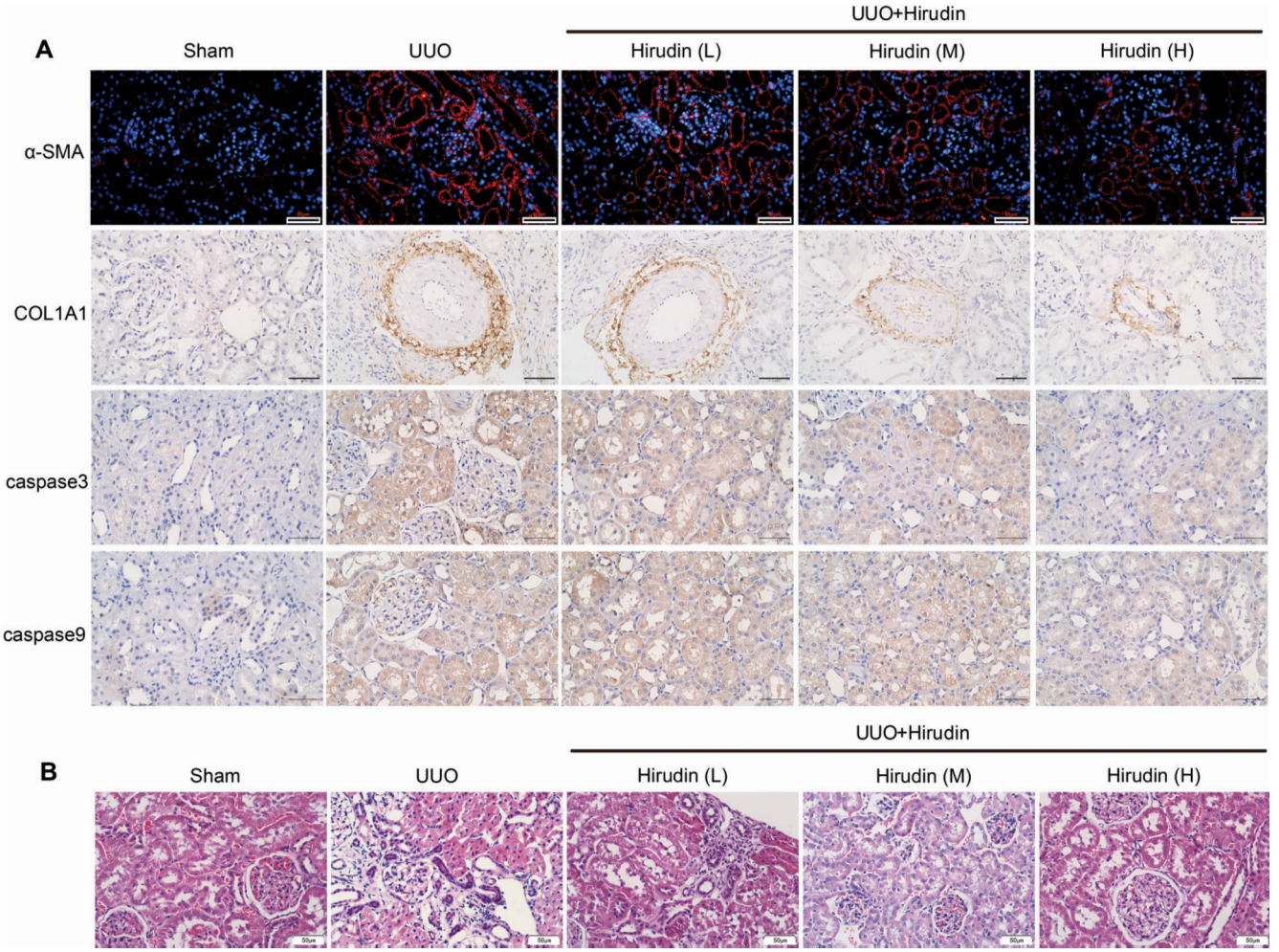

Figure 2. Effect of hirudin on renal fibrosis and apoptosis in UUO rats was investigated by immunofluorescence, immunohistochemistry, and H&E. **A**) Immunofluorescence was used to detect the level of α-SMA and immunohistochemistry was used to detect the levels of COL1A1, caspase-3, and caspase-9; scale bar: 50 μm. **B**) H&E staining for detection of RIF.

apoptosis. Compared to the Hirudin group, cell apoptosis in the Hirudin+sh HMGB1 group was significantly increased (Figure 4D). Immunofluorescence and IHC results showed that the level of α-SMA, COL1A1, caspase-3, and caspase-9 in the hirudin group was significantly lower than that in the NC group, and the level of α-SMA, COL1A1, caspase-3, and caspase-9 in the sh HMGB1 group was significantly lower than that in the sh NC group, indicating that hirudin and interference with HMGB1 can alleviate RIF. Compared to the Hirudin group, the level of α-SMA, COL1A1, caspase-3, and caspase-9 in the Hirudin+sh HMGB1 group was significantly increased (Figure 5A). HE staining results also showed an increased degree of renal tubular atrophy in the NC group, indicating the presence of significant renal injury. In the hirudin group, the degree of renal tubular dilatation, interstitial fibrosis and inflammatory cell infiltration was reduced. sh NC group showed no significant changes compared with NC group. sh HMGB1 group showed significantly less renal tubular atrophy than sh NC group, and the degree of interstitial fibrosis and inflammatory cell infiltration was reduced. The degree of renal tubular dilatation was significantly higher in the hirudin + sh HMGB1 group than in the hirudin group (Figure 5B).

Discussion

CKD, as a global health challenge, is increasingly prominent in terms of its high prevalence and severe harmfulness.[24] The pathogenesis of CKD is complex, with multiple factors jointly involved in the occurrence and development of the disease. In the early stage of CKD, tubular injury and interstitial fibrosis are the main pathological features, and the up-regulation of the expressions of α-SMA and COL1A1 are important markers of renal fibrosis.[25-28] Moreover, the imbalance between apoptosis and autophagy is also considered a key mechanism in the progression of CKD.[29] Existing studies have shown that abnormal autophagy can lead to podocyte loss, tubular cell injury, glomerulosclerosis, and other problems,

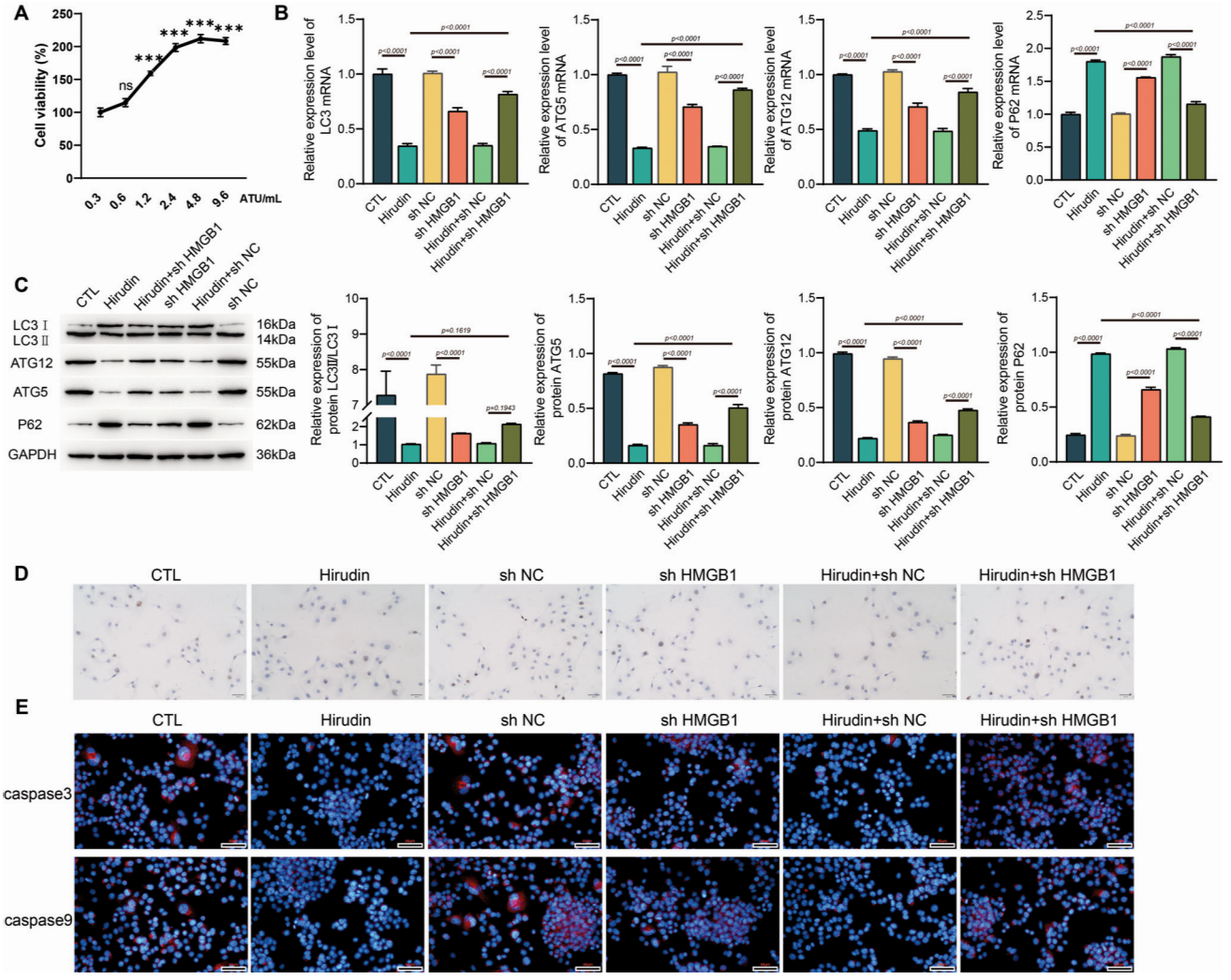

Figure 3. *In vitro* screening of the optimal effective concentration of hirudin and exploring the influence of hirudin and HMGB1 on CKD. **A**) The viability of HK-2 cells treated with different concentrations of hirudin detected by CCK-8. **B**) The expressions of LC3, ATG12, ATG5 and P62 mRNA in HK-2 cells was dected by RTqPCR. **C**) Western blot analysis of LC3-II/ LC3-I, ATG12, ATG5 and P62 protein levels in HK-2 cells. **D**) HK-2 cell apoptosis detection by TUNEL; scale bar: 50 μm. **E**) Immunofluorescence is showing the levels of caspase-3 and caspase-9.

thus accelerating the deterioration of CKD.[30] Moreover, the imbalance between apoptosis and autophagy is also considered a key mechanism in the progression of CKD

This study focused on the potential of hirudin, the main active component of the traditional Chinese medicine Hirudo, in the treatment of CKD. Previous studies have demonstrated that hirudin can reduce fibrin deposition in the glomeruli, inhibit mesangial cell proliferation, alleviate glomerulosclerosis, and enhance renal function.[32] Additionally, hirudin exhibits remarkable anti-inflammatory and anti-fibrotic functions.[33] The research by Deng *et al.*[34] indicated that hirudin could effectively inhibit the pro-inflammatory pathway, reduce the production of inflammatory factors, and suppress the development of renal fibrosis by decreasing the expressions of TGF-β1 and fibronectin 1 in renal tissues as well as the deposition of type IV collagen. Based on this, we hypothesized that the regulatory effect of hirudin on autophagy might be a key mechanism underlying its treatment of CKD.

In this study, we utilized a rat model of RIF constructed by UUO. We found that autophagy was abnormally activated in the RIF state, manifested as a significant up-regulation of autophagy-related genes and proteins such as LC3, ATG12, and ATG5, and a significant down-regulation of P62 expression. Meanwhile, the kidney coefficient in the model group increased significantly, apoptosis increased, and the levels of α-SMA, COL1A1, caspase-3, and caspase-9 were significantly elevated. These are all markers of aggravated RIF and apoptosis.[35-38] However, when treated with hirudin, the above-mentioned indicators were significantly improved. This indicates that hirudin can regulate abnormal autophagy levels, inhibit RIF and apoptosis, and thus exert a protective effect on renal function. Our research results are consistent with those of Yu *et al.*[22] After interfering with TGF-β in NRK-52E cells, autophagy was inhibited, and hirudin could reverse autophagic function and reduce the production of autophagy-related proteins such as P62, LC3, and Beclin-1.[22] The results of HE staining also showed that hirudin could reduce the degree of renal fibrosis in UUO rats, further supporting the hypothesis that hirudin

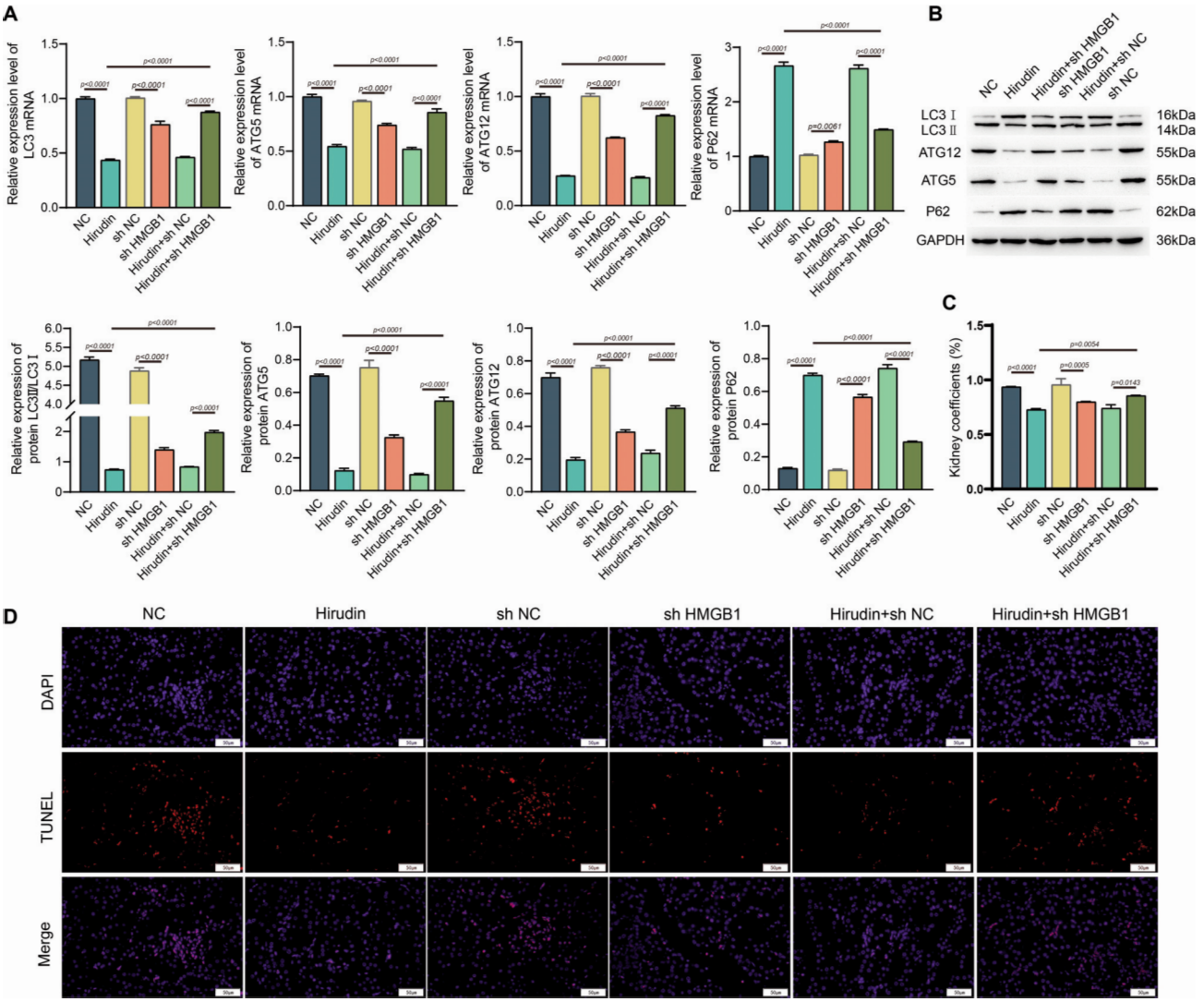

Figure 4. The effect of hirudin and HMGB1 in CKD rats was investigated in vivo. **A**) The expression of LC3, ATG12, ATG5 and P62 mRNAs in UUO rat kidney tissues verified by RTqPCR. **B**) Western blot analysis of LC3-II/ LC3-I, ATG12, ATG5 and P62 protein levels in UUO rat kidney tissue. **C**) Renal coefficient of UUO rat renal tissue. **D**) Apoptosis of kidney tissue in UUO rats was detected by TUNEL.

may protect renal function by regulating the autophagy process. Notably, the kidney coefficient of the hirudin-treated group was significantly lower than that of the model group, and the results of TUNEL staining showed that apoptosis in the hirudin-treated group was significantly reduced, further confirming the protective effect of hirudin on CKD. In addition, we experimented to screen the optimal concentration of hirudin for cells and determined that 4.8 ATU/mL was the optimal effective concentration of hirudin for HK-2 cells. The results of this study suggest that the autophagy activation induced by RIF may not be an effective protective response to renal injury, but may, to some extent, exacerbate renal lesions. Hirudin can correct this abnormally activated autophagy state and make the expression of autophagy-related proteins tend to be normal, which is consistent with the view in previous studies that moderate regulation of autophagy has a protective effect on the kidneys.[39,40] Excessive autophagy activation may lead to excessive degradation of intracellular substances, and impaired organelle function, and thus affect the normal physiological functions of cells.[41-43] By inhibiting excessive autophagy, hirudin maintains the stability of the intracellular environment and reduces the damage to renal cells, providing an important basis for explaining its role in the treatment of CKD.

Multiple clinical studies have confirmed that HMGB1 is closely associated with the onset, progression, and prognosis of CKD.[44-47] As a signaling molecule in the immune system, HMGB1 is widely regarded as a promoter of autophagy. Its release can trigger an inflammatory response and activate the TGF-β1/Smad2/3 signaling pathway, consequently leading to continuous damage to renal structure and function and accelerating the development of CKD.[48] Intracellularly, cytoplasmic HMGB1 is mainly involved in processes such as autophagy, mitochondrial function regulation, and programmed cell death.[49] The study by Martinez *et al*.[50] demonstrated that HMGB1 can directly regulate autophagy in leukemia cells by modulating the conversion of LC3 and can also indirectly promote autophagy by enhancing the functions of Beclin-1/PI3KC3 and Atg5-Atg12-Atg16. For example, a study found that HMGB1 can induce autophagy in bladder cancer cells, manifested as an increase in LC3-II and a decrease in P62.[51] In this study, we delved into the effects of hirudin and HMGB1 regulation on autophagy in CKD. The results showed that interfering with HMGB1 significantly reduced the expressions of LC3, ATG12, ATG5, LC3-II/LC3-I, caspase-3, and caspase-9, increased the level of P62, and decreased apoptosis. This result is similar to the findings of Mou *et al*.[31] in human melanocytes, where knocking out HMGB1 inhibited the expression of the autophagy marker LC3, enhanced the expression of P62, and inhibited both autophagy and apoptosis.[31] Moreover, when the expression of HMGB1 was interfered with, the therapeutic effect of hirudin declined. The expression levels of LC3, ATG12, ATG5, LC3-II/LC3-I, caspase-3, and caspase-9 increased, the expression of P62 decreased, and apoptosis increased. This result indicates that the therapeutic effect of hirudin is closely related to HMGB1. Interfering with HMGB1 weakens the regulatory effects of hirudin on autophagy, apoptosis, and RIF, suggesting that hirudin may exert its therapeutic effect on CKD by influencing HMGB1-related pathways. However, this study has certain limitations. In terms of mechanism research, although the associations among hirudin, HMGB1, autophagy, and apoptosis have been clarified, the specific molecular signaling pathways have not been fully elucidated. Additionally, this study was only based on animal models and cell experiments and lacks verification from large - scale clinical studies. Meanwhile, the

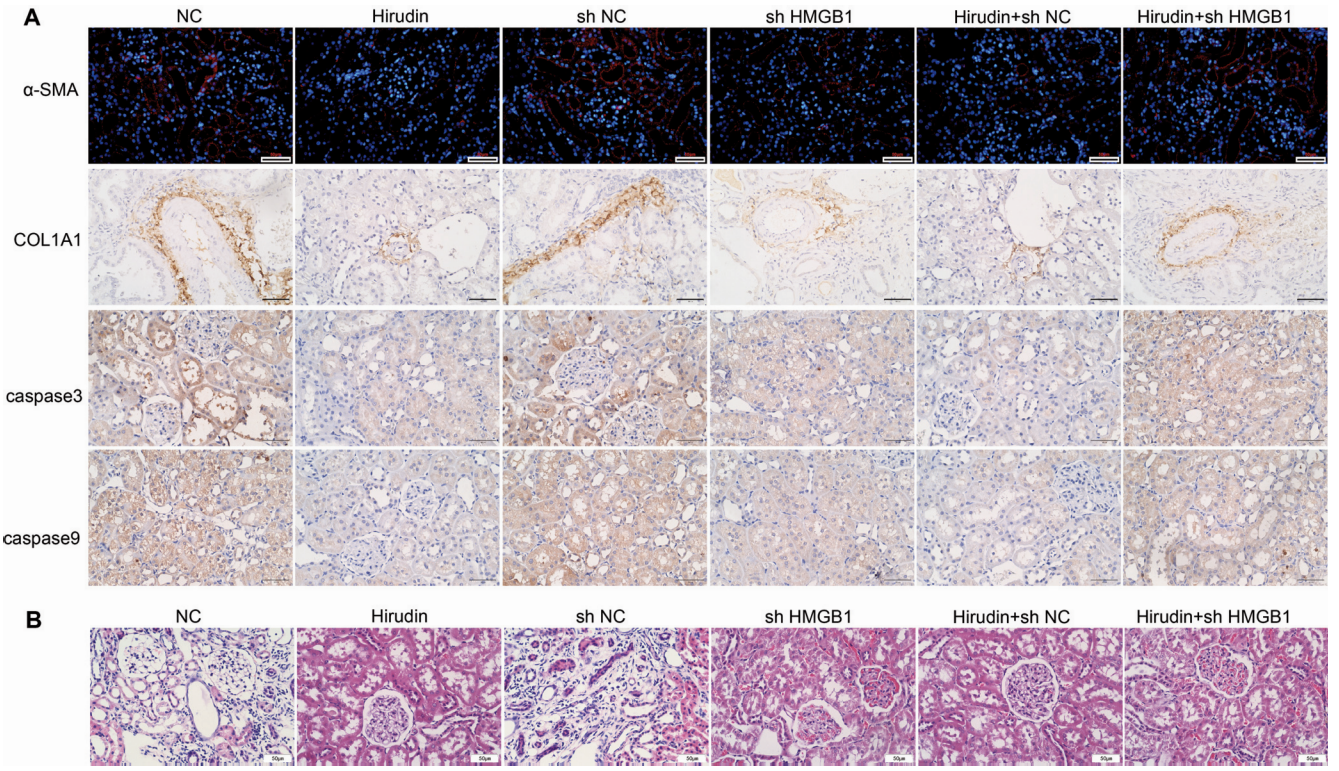

Figure 5. The effect of hirudin and HMGB1 in CKD rats was investigated by immunofluorescence, immunohistochemistry, and H&E. **A**) Immunofluorescence detection of the level of α-SMA and IHC detection of the level of COL1A1, caspase-3, and caspase-9. **B**) H&E staining for detection of RIF.

impact of CKD caused by different etiologies on the therapeutic effect of hirudin was not considered in experiments. CKD triggered by different causes may have different pathophysiological mechanisms, which may lead to differences in the therapeutic effects of hirudin and should be paid attention to in future research. Therefore, this study not only confirms the efficacy of hirudin and its regulatory role in cellular autophagy but also reveals the potential impact of hirudin on HMGB1 and its significance in the treatment of CKD. These findings are of great significance for the development of novel therapies for CKD, providing new insights and strategies for clinical treatment. However, there are still some limitations in the study, such as the validation of hirudin's effects only in animal models, and more research support is needed for clinical application. Future research directions could include further exploration of the interaction and mechanism between hirudin and HMGB1, conducting more clinical trials to validate its effectiveness, and delving into the specific pathways of hirudin in CKD treatment, providing more innovative breakthroughs for the management of CKD.[30,31]

References

1. Andrassy KM. Comments on 'kdigo 2012 clinical practice guideline for the evaluation and management of chronic kidney disease'. Kidney Int 2013;84:622-3.
2. Lameire NH, Levin A, Kellum JA, Cheung M, Jadoul M, Winkelmayer WC, et al. Harmonizing acute and chronic kidney disease definition and classification: Report of a kidney disease: Improving global outcomes (kdigo) consensus conference. Kidney Int 2021;100:516-26.
3. Lin TA, Wu VC, Wang CY. Autophagy in chronic kidney diseases. Cells 2019;8:61.
4. Yasukochi Y, Sakuma J, Takeuchi I, Kato K, Oguri M, Fujimaki T, et al. Identification of cdc42bpg as a novel susceptibility locus for hyperuricemia in a japanese population. Mol Genet Genomics 2018;293:371-9.
5. Liu HF, Yang JW. Chinese expert consensus on autophagy and kidney disease research. Chin J Pathophysiol 2021;37:1876-87.
6. Feng C, Yuan X. Role of autophagy and its regulation by noncoding rnas in ovarian cancer. Exp Biol Med (Maywood) 2023;248:1001-12.
7. Ruan GP, Xu F, Li ZA, Zhu GX, Pang RQ, Wang JX, et al. Induced autologous stem cell transplantation for treatment of rabbit renal interstitial fibrosis. PLoS One 2013;8:e83507.
8. Li X, Bu X, Yan F, Wang F, Wei D, Yuan J, et al. Deletion of discoidin domain receptor 2 attenuates renal interstitial fibrosis in a murine unilateral ureteral obstruction model. Ren Fail 2019;41:481-8.
9. Huan HD, Zhang JH, Zheng SR, Meng WW, Zhang JL. [Dilingdan decoction prevents renal interstitial fibrosis in a rat model of unilateral ureteral obstruction].[Article in Chinese] Zhong Xi Yi Jie He Xue Bao 2008;6:493-7.
10. Wang WW, Liu YL, Wang MZ, Li H, Liu BH, Tu Y, et al. Inhibition of renal tubular epithelial mesenchymal transition and endoplasmic reticulum stress-induced apoptosis with Shenkang injection attenuates diabetic tubulopathy. Front Pharmacol 2021;12:662706.
11. Xin L, Jing X, Li H, Wenfan G, Ming C. Efficacy and safety of activating blood circulation and removing blood stasis of traditional chinese medicine for managing renal fibrosis in patients with chronic kidney disease: A systematic review and meta-analysis. J Tradit Chin Med 2023;43:429-40.
12. Yao M, Qin S, Xiong J, Xin W, Guan X, Gong S, et al. Oroxylin a ameliorates aki-to-ckd transition through maintaining pparα-bnip3 signaling-mediated mitochondrial homeostasis. Front Pharmacol 2022;13:935937.
13. Zhu J, Pan X, Lin B, Lin G, Pradhan R, Long F, et al. The effect of hirudin on antagonisting thrombin induced apoptosis of human microvascular endothelial cells1. Acta Cir Bras 2019;34:e20190010000006.
14. Ying-Xin G, Guo-Qian Y, Jia-Quan L, Han X. Effects of natural and recombinant hirudin on superoxide dismutase, malondialdehyde and endothelin levels in a random pattern skin flap model. J Hand Surg Eur Vol 2012;37:42-9.
15. Lu Y, Yang RC, Zhu XL, Wang YJ, Wang J. The effect of ox-ldl induced activated macrophages on the expression of TGF-β and FN gene in glomerular mesangial cells and the intervention effect of hirudin. Chin J Integr Nephrol 2007:631-3.
16. Han J, Zuo Z, Shi X, Zhang Y, Peng Z, Xing Y, et al. Hirudin ameliorates diabetic nephropathy by inhibiting gsdmd-mediated pyroptosis. Cell Biol Toxicol 2023;39:573-89.
17. Li Y, Cui L. Clinical study of hirudin in the treatment of diabetic nephropathy and hypertensive nephropathy with urinary microalbumin as the main manifestation. Journal of Clinical Rational Drug Use 2010;3:2.
18. Yang K, Cao F, Wang W, Tian Z, Yang L. The relationship between hmgb1 and autophagy in the pathogenesis of diabetes and its complications. Front Endocrinol (Lausanne) 2023;14:1141516.
19. Oh H, Choi A, Seo N, Lim JS, You JS, Chung YE. Protective effect of glycyrrhizin, a direct hmgb1 inhibitor, on post-contrast acute kidney injury. Sci Rep 2021;11:15625.
20. Zhao J, Sun T, Wu S, Liu Y. High mobility group box 1: An immune-regulatory protein. Curr Gene Ther 2019;19:100-9.
21. Tang D, Kang R, Cheh CW, Livesey KM, Liang X, Schapiro NE, et al. Hmgb1 release and redox regulates autophagy and apoptosis in cancer cells. Oncogene 2010;29:5299-310.
22. Yu HX, Lin W, Yang K, Wei LJ, Chen JL, Liu XY, et al. Transcriptome-based network analysis reveals hirudin potentiates anti-renal fibrosis efficacy in uuo rats. Front Pharmacol 2021;12:741801.
23. Wang M, Dai M, Wu YS, Yi Z, Li Y, Ren G. Immunoglobulin superfamily member 10 is a novel prognostic biomarker for breast cancer. PeerJ 2020;8:e10128.
24. Adapala NS, Root S, Lorenzo J, Aguila H, Sanjay A. Pi3k activation increases sdf-1 production and number of osteoclast precursors, and enhances sdf-1-mediated osteoclast precursor migration. Bone Rep 2019;10:100203.
25. Arseni L, Lombardi A, Orioli D. From structure to phenotype: Impact of collagen alterations on human health. Int J Mol Sci 2018;19:1407.
26. Jin J, Wang T, Park W, Li W, Kim W, Park SK, et al. Inhibition of yes-associated protein by verteporfin ameliorates unilateral ureteral obstruction-induced renal tubulointerstitial inflammation and fibrosis. Int J Mol Sci 2020;21:8184.
27. Hoshino J, Mise K, Ueno T, Imafuku A, Kawada M, Sumida K, et al. A pathological scoring system to predict renal outcome in diabetic nephropathy. Am J Nephrol 2015;41:337-44.
28. Chawla LS, Eggers PW, Star RA, Kimmel PL. Acute kidney injury and chronic kidney disease as interconnected syndromes. N Engl J Med 2014;371:58-66.
29. Quaglia M, Merlotti G, Fornara L, Colombatto A, Cantaluppi V. Extracellular vesicles released from stem cells as a new therapeutic strategy for primary and secondary glomerulonephritis. Int J Mol Sci 2022;23:5760.
30. Yuan S, Liu Z, Xu Z, Liu J, Zhang J. High mobility group box 1 (hmgb1): A pivotal regulator of hematopoietic malignancies. J Hematol Oncol 2020;13:91.

31. Mou K, Liu W, Miao Y, Cao F, Li P. Hmgb1 deficiency reduces h(2) o(2) -induced oxidative damage in human melanocytes via the nrf2 pathway. J Cell Mol Med 2018;22:6148-56.
32. Cui H, Fu FQ, Liu B, Liu WJ, Liu YN. Herbal medicine "shulifenxiao" formula for nephrotic syndrome of refractory idiopathic membranous nephropathy. Front Pharmacol 2021;12:675406.
33. Müller C, Haase M, Lemke S, Hildebrandt JP. Hirudins and hirudin-like factors in hirudinidae: Implications for function and phylogenetic relationships. Parasitol Res 2017;116:313-25.
34. Deng F, Zhang J, Li Y, Wang W, Hong D, Li G, et al. Hirudin ameliorates immunoglobulin a nephropathy by inhibition of fibrosis and inflammatory response. Ren Fail 2019;41:104-12.
35. Wang L, Li X, Hanada Y, Hasuzawa N, Moriyama Y, Nomura M, et al. Dynamin-related protein 1 deficiency accelerates lipopolysaccharide-induced acute liver injury and inflammation in mice. Commun Biol 2021;4:894.
36. Barbaro JM, Cuervo AM, Berman JW. Hiv increases the inhibitory impact of morphine and antiretrovirals on autophagy in primary human macrophages: Contributions to neuropathogenesis. Cells 2021;10:2183.
37. Zhou J, Zhang C, Fang X, Zhang N, Zhang X, Zhu Z. Activation of autophagy inhibits the activation of nlrp3 inflammasome and alleviates sevoflurane-induced cognitive dysfunction in elderly rats. BMC Neurosci 2023;24:9.
38. Shang C, Zhuang X, Zhang H, Li Y, Zhu Y, Lu J, et al. Inhibition of autophagy suppresses sars-cov-2 replication and ameliorates pneumonia in hace2 transgenic mice and xenografted human lung tissues. J Virol 2021;95:e0153721.
39. Ma Y, Wu S, Zhao F, Li H, Li Q, Zhang J, et al. Hirudin inhibits glioma growth through mtor-regulated autophagy. J Cell Mol Med 2023;27:2701-13.
40. Xiang Y, Fu Y, Wu W, Tang C, Dong Z. Autophagy in acute kidney injury and maladaptive kidney repair. Burns Trauma 2023;11:tkac059.
41. Chen Y, Zhao Y, Mishra PK. Editorial: Autophagy-mediated cell survival and death in disease progression and treatment. Front Cell Dev Biol 2022;10:916347.
42. Debnath J, Gammoh N, Ryan KM. Autophagy and autophagy-related pathways in cancer. Nat Rev Mol Cell Biol 2023;24:560-75.
43. Liu SJ, Cao YL, Zhang C. Hirudin in the treatment of chronic kidney disease. Molecules 2024;29:1029.
44. Rui-Zhi T, Hui D, Jian-Chun L, Xia Z, Xiao-Jia W, Dan W, et al. Astragalus mongholicus bunge and panax notoginseng formula (a&p) combined with bifidobacterium contribute a renoprotective effect in chronic kidney disease through inhibiting macrophage inflammatory response in kidney and intestine. Front Physiol 2020;11:583668.
45. Geuens T, van Blitterswijk CA, LaPointe VLS. Overcoming kidney organoid challenges for regenerative medicine. NPJ Regen Med 2020;5:8.
46. Jin X, Rong S, Yuan W, Gu L, Jia J, Wang L, et al. High mobility group box 1 promotes aortic calcification in chronic kidney disease via the Wnt/β-catenin pathway. Front Physiol 2018;9:665.
47. Sato F, Maruyama S, Hayashi H, Sakamoto I, Yamada S, Uchimura T, et al. High mobility group box chromosomal protein 1 in patients with renal diseases. Nephron Clin Pract 2008;108:c194-201.
48. Leelahavanichkul A, Huang Y, Hu X, Zhou H, Tsuji T, Chen R, et al. Chronic kidney disease worsens sepsis and sepsis-induced acute kidney injury by releasing high mobility group box protein-1. Kidney Int 2011;80:1198-211.
49. Zhou S, Yu Z, Chen Z, Ning F, Hu X, Wu T, et al. Olmesartan alleviates sars-cov-2 envelope protein induced renal fibrosis by regulating hmgb1 release and autophagic degradation of tgf-β1. Front Pharmacol 2023;14:1187818.
50. Martinez J, Almendinger J, Oberst A, Ness R, Dillon CP, Fitzgerald P, et al. Microtubule-associated protein 1 light chain 3 alpha (lc3)-associated phagocytosis is required for the efficient clearance of dead cells. Proc Natl Acad Sci USA 2011;108:17396-401.
51. Yin H, Yang X, Gu W, Liu Y, Li X, Huang X, et al. Hmgb1-mediated autophagy attenuates gemcitabine-induced apoptosis in bladder cancer cells involving jnk and erk activation. Oncotarget 2017;8:71642-56.

Received: 3 January 2025. Accepted: 7 March 2025.

European Journal of Histochemistry 2025; 69:4182
doi:10.4081/ejh.2025.4182